

Article

Nanoparticle-Induced Changes in Resistance and Resilience of Sensitive Microbial Indicators towards Heat Stress in Soil

Abhishek Kumar ¹, Rajiv Rakshit ¹, Arnab Bhowmik ^{2,*} , Nintu Mandal ¹, Anupam Das ^{1,*} 
and Samrat Adhikary ^{1,†}

¹ Department of Soil Science and Agricultural Chemistry, Bihar Agricultural University, Bihar Sabour 813 210, India; abhishek.3881@gmail.com (A.K.); rajiv.ssaciari@gmail.com (R.R.); nintumandal@gmail.com (N.M.); samratadhikarysoil@gmail.com (S.A.)

² Department of Natural Resources and Environmental Design, North Carolina A&T State University, Greensboro, NC 27411, USA

* Correspondence: abhowmik@ncat.edu (A.B.); anusoil22@gmail.com (A.D.)

† Present address: Department of Agricultural Chemistry and Soil Science, BCKV, Mohanpur, West Bengal Nadia 741 252, India.

Received: 20 December 2018; Accepted: 2 February 2019; Published: 7 February 2019



Abstract: Modern agricultural innovations with nanomaterials are now being applied in every sphere of agriculture. However, their interaction with soil microbial processes is not being explored in detail. This initiative was undertaken to understand the effect of metal-oxide nanoparticles with heat stress in soil. Metal-oxide nanoparticles, zinc oxide (ZnO), and iron oxide (Fe₂O₃) (each at 10 and 40 mg kg⁻¹ w/w) were mixed into uncontaminated soil and subjected to heat stress of 48 °C for 24 hours to assess their effect on soil biological indicators. The resistance indices for the acid (ACP), alkaline phosphatase (AKP) activity, and fluorescein diacetate hydrolyzing (FDA) activity (0.58 to 0.73, 0.58 to 0.66, and 0.42 to 0.48, respectively) were higher in the presence of ZnO nanoparticles as compared to Fe₂O₃ nanomaterials, following an unpredictable pattern at either 10 or 40 mg kg⁻¹ in soils, except dehydrogenase activity (DHA), for which the activity did not change with ZnO nanomaterial. An explicit role of ZnO nanomaterial in the revival pattern of the enzymes was observed (0.20 for DHA, 0.39 for ACP, and 0.43 for AKP), except FDA, which showed comparable values with Fe₂O₃ nanomaterials for the following 90 day (d) after stress. Microbial count exhibiting higher resistance values were associated with Fe₂O₃ nanoparticles as compared to ZnO nanomaterials, except *Pseudomonas*. The recovery indices for the microbial counts were higher with the application of Fe₂O₃ nanomaterials (0.34 for Actinobacteria, 0.38 for fungi, 0.33 for *Pseudomonas* and 0.28 for *Azotobacter*). Our study emphasizes the fact that sensitive microbial indicators in soil might be hampered by external stress initially but do have the competency to recover with time, thereby reinstating the resistance and resilience of soil systems.

Keywords: heat stress; microbial count; zinc and iron oxide nanoparticles; resistance; restoration; soil enzymes

1. Introduction

Nanomaterials are being increasingly used owing to their exclusive properties (high aspect ratio; surface area to volume ratio) making them valuable for copious agricultural applications. Based on the mode of application, there is every possibility of its entry into the soil system and directly or indirectly interacting with a range of soil components. Soil is a major environmental compartment considered as a sink for these materials, which is of serious concern because of their typical dissolution properties

and charges, in addition to their small sizes and large surface-to-mass ratios [1]. Numerous studies have shown that exposure to external nanomaterials can be toxic for microbes [2]. Toxic effects of these particles have been observed in several in vitro studies; in particular, many nanoparticles, such as zinc-oxide nanoparticles, are known to have antimicrobial properties [3]. Jiang et al. [4] found that engineered ZnO nanoparticles were toxic, causing 100% mortality of *B. subtilis*, *E. coli*, and *P. fluorescens*. Conversely, Dimkpa et al. [5] reported that CuO nanoparticles were more noxious to the beneficial rhizosphere isolate *P. Chlororaphis* than ZnO nanoparticles. The toxicity mechanism involves oxidative stress generated by the fabrication of reactive oxygen species (ROS) from nanoparticles in contact with microbial membranes, causing disruption of membranes, oxidation of proteins, or interruption of energy transduction [6]. Pawlett et al. [7] studied the impact of nanosized zero-valent iron, an effective land remediation tool, on soil microbial biomass in an incubation experiment with three soil textural class types and reported that the zero-valent iron significantly reduced microbial biomass by 29%. Effects of nanoscale and microscale zero-valent iron particles on ammonia oxidation potential usually mediated by microorganisms showed an inhibition in its potential, suggesting possible changes in the microbial community. Nanoscale and microscale zero-valent iron particles stimulated dehydrogenase activity (DHA), but had minimal influence on hydrolase activity [8]. These results indicate that metal and metal oxides can induce modification of microbial activities in soil and of biogeochemical cycles. However, reports on the relative toxicities of these metal and metal-oxide nanoparticles on soil microorganisms are contradictory and vary according to the type of nanoparticles, their concentrations, contact time, and activity. Although several previous works related to the influence of nanomaterials on microorganisms exist in the literature, we could not locate studies focusing on the impact of nanomaterials on the resistance and recovery of these soil organisms (in terms of their number, biomass, and associated enzymes) under abiotic stresses such as heat.

Aberrations in atmospheric temperatures were observed in the last two decades, which can influence soil organisms and microbial processes [9]. Behavior of synthetic nanomaterials needs to be evaluated as to whether nanoparticles can be potentially utilized in the agricultural sector to combat the ill effects of changing climate on soils and microorganisms therein, ultimately benefitting crop productivity. It is quite obvious that stresses (high temperature or addition of nanomaterials) of this nature may have large impact on soil microorganisms, which are considered to be the key players in soil functions. In order to significantly maintain these soil functions, the response of soils to stress has therefore become a focal point of ecological research. Resistance (the capacity of a soil to function) and resilience (ability to counteract adverse changes) are the key terms that can be considered as indicators of ecological stability and are related to soil health [10]. Resistance and resilience are highly correlated to the diversity of microbial communities and properties of the inherent soil organisms [11]. Considering heat as an abiotic stress, in this study, we hypothesized that addition of nanomaterials could have considerable implications on these soil microflora and enzymes and also influence the resistance and resilience of soil organisms against high temperature. To test this hypothesis, an incubation experiment was conducted to evaluate the abundance of microbial groups, microbial biomass, and enzyme activities in soils amended with nanomaterials and elucidate the resistance and resilience of soil microbes and associated enzymes against heat stress. A review of the global literature revealed that the impact of nanomaterials on the soil microbial community is context-dependent (nature, type of nanomaterials, dose, soil types, types of microbes, etc.). Thorough scientific study on the impact assessment of nanomaterials on the soil microbial community and its trend prediction are necessary to understand the behavior of organisms and associated soil enzymes.

2. Material and Methods

2.1. Site Description and Soil Sampling

The experiment was conducted with soil obtained from a permanent plot experiment, which was established in 1984 at the Bihar Agricultural College Research Farm (25°23'N, 87°07'E, 37.19 mean sea

level), under the network project research program of the Indian Institute of Farming System Research, Modipuram, India. The soil texture is clayey with the following physico-chemical properties: pH: 7.40, organic carbon: 0.46%, available nitrogen: (N) 194 kg ha⁻¹, available phosphorus (P): 10.12 kg ha⁻¹, and available potassium (K): 128.65 kg ha⁻¹. The experiment was laid out in randomized block design with 4 replicates with the following treatments: control (T₁) (no fertilizer, no organic manure); 50% recommended dose of fertilizers (RDF) to both rice and wheat (T₂); 50% RDF to rice and 100% RDF to wheat (T₃); 75% RDF to both rice and wheat (T₄); 100% RDF to both rice and wheat (T₅); 50% RDF + 50% N through farm yard manure (FYM) to rice and 100% RDF to wheat (T₆); 75% RDF + 25% N through FYM to rice and 75% RDF to wheat (T₇); 50% RDF + 50% N through wheat straw to rice and 100% RDF to wheat (T₈); 75% RDF + 25% N through wheat straw to rice and 75% RDF to wheat (T₉); 50% RDF + 50% N through green leaf manure (GLM) (*Sesbaniaaculeata*) to rice and 100% RDF to wheat (T₁₀); 75% RDF + 25% N through GLM to rice and 75% RDF to wheat (T₁₁); farmers' fertilizers practice to rice and wheat (70 kg N + 13.2 kg P + 8.3 kg ha⁻¹)(T₁₂). Soils (0–15-cm depth) were sampled from the control plots after harvest of rice crop (October) in 2015 in order to ensure that samples were not contaminated either with fertilizers or any supplementary materials. Using a soil core (inner diameter: 4.8 cm and height: 15 cm), a total of 32 random samples were collected from 4 field replicates to form a composite sample.

2.2. Synthesis of Zinc-Oxide (ZnO) Nanoparticles

The ZnO nanoparticles were synthesized following the procedure outlined by Aneesh et al. [12]. In order to synthesize the ZnO nanoparticles, stock solutions of Zn (CH₃COO)₂ 2H₂O (0.1 M) was prepared in 50 mL methanol under stirring. Then, 25 mL of NaOH (varying from 0.2 M to 0.5 M, solution prepared in methanol) was added to the stock solution with constant stirring in order to raise the pH value of reactants to 10. These solutions were transferred into Teflon-lined sealed stainless steel autoclaves and maintained at various temperature in the range of 100–200 °C for 6 and 12 h under autogenous pressure. Solutions were then allowed to cool naturally to room temperature. The synthesized samples were characterized for their structure by X-ray diffraction (XRD) and transmission electron microscopy (TEM).

2.3. Synthesis of Iron-Oxide (Fe₂O₃) Nanoparticles

The Fe₂O₃ nanoparticles were synthesized following standard procedure as outlined by Shah and Shah [13]. A solution of 0.6 M NaOH was prepared in double-distilled water and 0.01 M solution of FeCl₃ was added into it. Stirring was continued up to 30 min, maintaining constant temperature at 100 °C, and a precipitate of Fe(OH)₃ was obtained. It was washed with double-distilled water several times until the pH became 8.8. Then, 1 mL of 1 M HCl and 10 mL of 0.1 M solution of NaH₂PO₄ was added to the precipitate, stirred, and heated up to 100 °C. Iron-oxide particles formed were filtered, washed within distilled water, and dried in air. The particles were also characterized by TEM and XRD.

2.4. Characterization of ZnO and Fe₂O₃ Nanoparticles by TEM and XRD

TEM images of ZnO and Fe₂O₃ nanoparticles were taken through a TEM manufactured by JEOL, Japan (JEN 1011, 100 KV). Specific instrumental setup was 80 kV HV with magnification 80,000×. Powder diffractions of ZnO and Fe₂O₃ were taken and scanned separately in a Philips PW 1710 X-ray diffractometer using automated powder diffraction (APD) software (PAN analytical, Spectris Technologies), with the setting of the instruments as follows: radiation type: Cu Kα; tube current: 20 mA; generator voltage: 40 kV; start angle (°2θ): 3.00; end angle (°2θ): 40.00; scan step size: 0.1; scan type: continuous; scan speed (2θ Sec⁻¹): 0.025. Mineralogy of Fe₂O₃ and ZnO nanoparticles were confirmed through powder diffraction data from the Joint Committee on Powder Diffraction Standards (JCPDS) [14].

2.5. Average Crystalline Size Calculation

Average crystalline size of ZnO and Fe₂O₃ nanoparticles were estimated using the Debye–Scherrer formula [15] as presented below:

$$D = \frac{0.9 \lambda}{\beta \cos \theta}$$

where λ represents the wave length of X-rays (0.1541 nm), β is FWHM (full width at half maximum), θ is the diffraction angle, and D is the particle diameter size.

2.6. Incubation Experiment Details

To test the effect of nanomaterials on the resistance and resilience of the microbial parameters, the control soil was treated with two novel materials—zinc and iron nanomaterials—each at 10 and 40 mg kg^{−1} and kept uniformly for 30 d before incubation to establish equilibrium. Biological indicators were assessed thereafter and considered as the values for day 0. After 30 d, samples were subjected to stress by incubating them at 48 °C for 24 h. Thereafter, soils were brought back to the moisture content at 60% of maximum water holding capacity to measure their resilience. Moisture content at this level resembles the field capacity of soil considered indispensable for the recovery of microbes and hence associated enzymes. Once the moisture content of 18–20% (v/v) was achieved, the samples were incubated at 28 ± 2 °C for measuring the soil parameters at 1, 14, 28, 56, 70, and 90 d after stress [16]. Once the data on various parameters were measured, the resistance and resilience indices of the measured parameters were calculated (see Section 2.8).

2.7. Biological Indicators of Soil Health

The DHA in soil was determined by the spectrophotometric method as described by Klein et al. [17] using 3% triphenyl tetrazolium chloride (TTC). Of the various methods available for assay of phosphomonoesterase activity, i.e., acid phosphatase (ACP) and alkaline phosphatase (AKP) in soils, the method of Tabatabai and Bremner [18] is the most rapid, accurate, and precise. Fluorescein diacetate activity (FDA) activity in soils was determined by the methodology as described by Green et al. [19]. For this purpose, 1 g of air-dried soil was taken in a 125 mL Erlenmeyer flask and 50 mL of 60 mM sodium phosphate buffer (pH 7.6) and 0.50 mL of 4.9 mM FDA lipase substrate solution (20 mg FDA lipase substrate in 10 mL acetone) were added to the flasks. The absorbance was measured on a spectrophotometer at a wavelength of 490 nm. Soil microbial biomass carbon (MBC) was analyzed by the procedure given by Vance et al. [20] using 0.5M K₂SO₄ as an extractant. The MBC was calculated using the formula given below and reported on an oven-dried soil basis.

$$MBC \left(mg \ C \ kg^{-1} \ Soil \right) = \frac{C_F - C_{UF}}{K_{EC}}$$

where C_F:carbon in fumigated soil, C_{UF}:carbon in unfumigated soil, and K_{EC}:efficiency of extraction (0.45).

Serial dilutions were prepared within the laminar flow assembly for counting and isolation of soil Actinobacteria, fungi, *Pseudomonas*, and *Azotobacter* [21].

2.8. Measurement of Resistance and Resilience Indices

The resistance index calculates the absolute amount of change relative to the control at the end of the disturbance [22] and ranges from −1 to +1, with +1 indicating maximum resistance (that is, no effect of stress). The resilience index calculates the absolute difference that exists between stress and control treatments relative to the initial absolute effect of the disturbance and ranges from −1 to +1,

with +1 indicating maximum resilience (that is, complete recovery after rewetting) [11]. The formulas used for calculating resistance and resilience are given below:

$$RS \text{ at } t_0 = 1 - \frac{|2D_0|}{(C_0 + |D_0|)} \quad (1)$$

$$RL \text{ at } t_x = \frac{|2D_0|}{(|D_0| + |D_x|)} - 1 \quad (2)$$

where, D_0 is the difference between the control (C_0) and the disturbed soil at the end of disturbance (t_0) and D_x is the difference between the control and the disturbed soil at the time point (t_x).

2.9. Statistical Analysis

Data obtained from the experiment with a completely randomized design was statistically analyzed by analysis of variance (ANOVA) using Microsoft Excel (Microsoft Corporation, USA) and SPSS window version 16.0 (SPSS Inc., Chicago, IL, USA) packages to ascertain the treatment effect [23]. Duncan's multiple range test (DMRT) was carried out for mean comparison, where ANOVA was significant at $p < 0.05$. The Pearson's correlation among various parameters was done as the sample was large ($n = 105$) through SPSS 16.0 software.

3. Results

3.1. Characterization of Synthesized Nanomaterials

The synthesized nanomaterials (Fe_2O_3 and ZnO) were characterized through TEM and XRD. The diameter of synthesized Zn and Fe oxides were 44.14–67.61 nm and 39.73–45.50 nm, respectively (Figures 1 and 2), which confirms that synthesized materials are in the nanoscale range. XRD study (Figures 3 and 4) confirms the wurtzite crystal structure, which signifies the stability of the materials. Crystal structure of Zn- and Fe-oxide nanoparticles were confirmed through respective typical XRD peaks in comparison with the JCPDS profile.

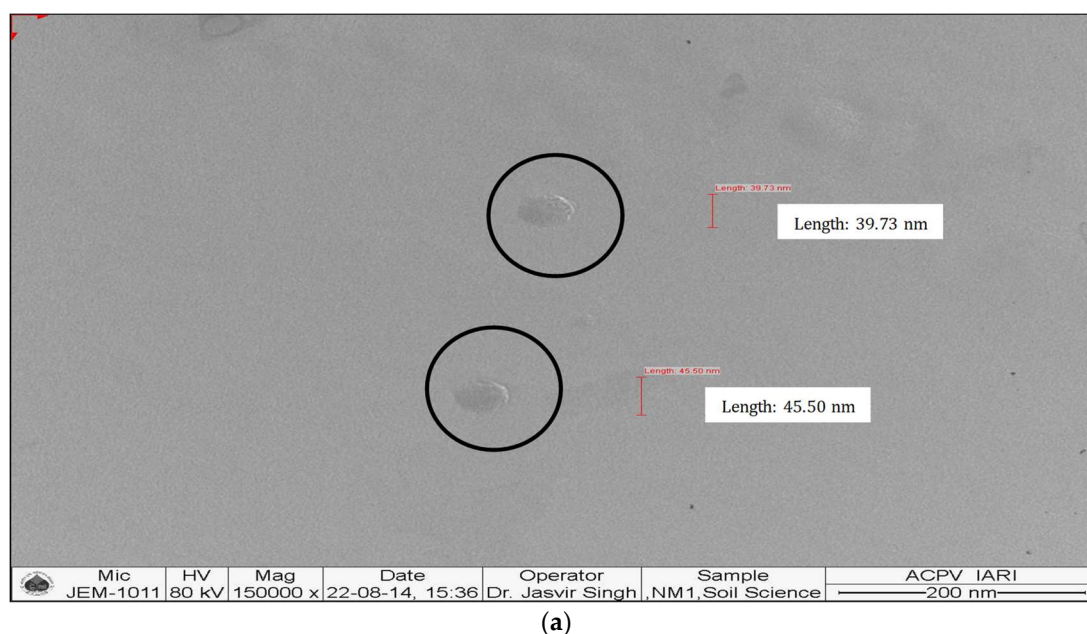
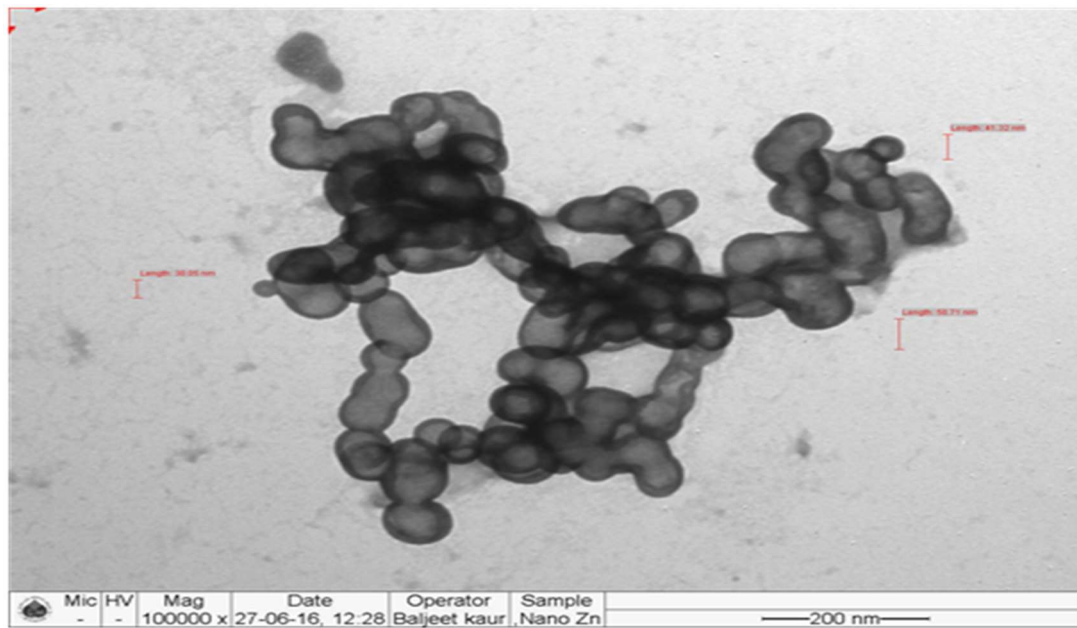
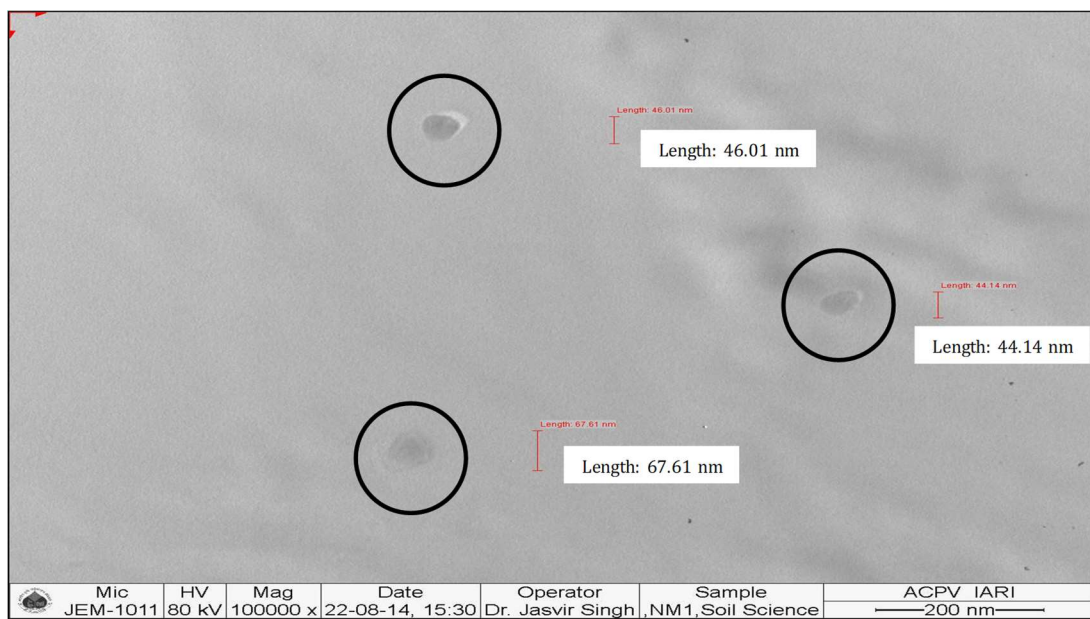


Figure 1. Cont.



(b)

Figure 1. Transmission electron microscopy (TEM) images of ZnO nanoparticles, (a) size and (b) shape.



(a)

Figure 2. Cont.

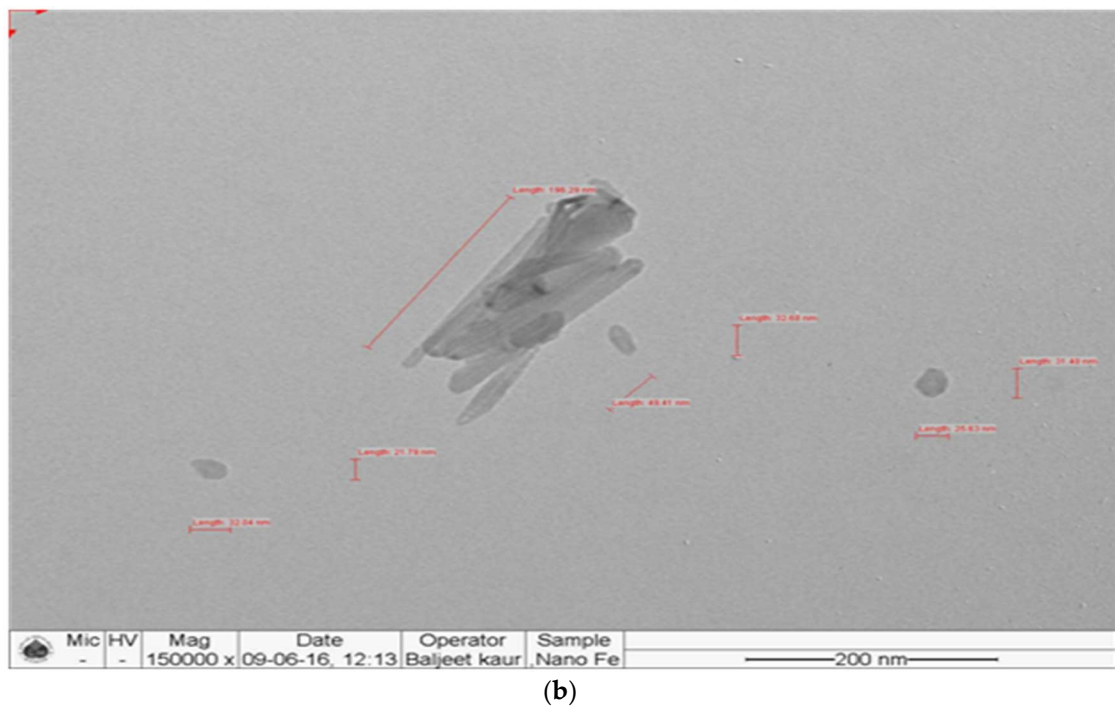


Figure 2. Transmission electron microscopy (TEM) images of Fe₂O₃ nanoparticles, (a) size and (b) shape.

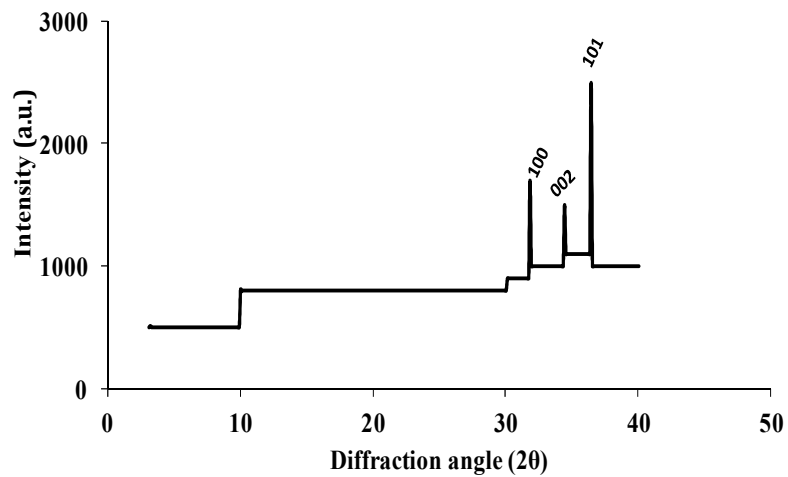


Figure 3. X-ray diffraction (XRD) results for ZnO nanoparticles where 100, 002 and 101 are Miller Indices for ZnO nanoparticles.

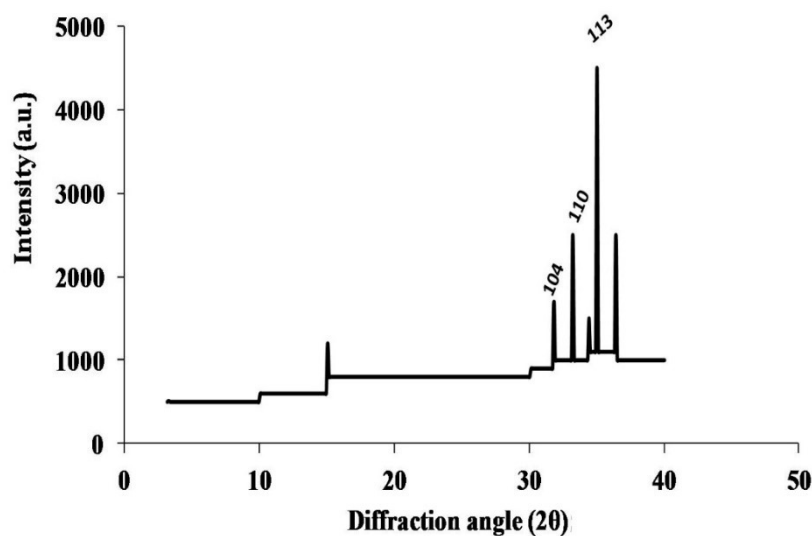


Figure 4. X-ray diffraction (XRD) results for Fe_2O_3 nanoparticles, where 104, 110 and 113 are Miller Indices for Fe_2O_3 nanoparticles.

3.2. Biological Indicators of Soil Health

Across all the treatments, DHA in soil on day 0 (0 d) ranged from 17.61 to 24.34 μg triphenyl formazan (TPF) released g^{-1} dry soil h^{-1} . DHA was significantly ($p < 0.05$) higher in the control (24.34 μg TPF released g^{-1} dry soil h^{-1}) than the treatments with nanomaterials added (T_2 to T_5) (18.78–20.26 μg TPF released g^{-1} dry soil h^{-1}), showing the toxic effect of these materials on the metabolic activity of the microorganisms in soil. In comparison to the control, data revealed a decrease of the DHA by 20 to 38% with the addition of these nanomaterials (Figure 5). The ACP activity was significantly lower in treatment T_3 (81.61 μg p-nitrophenol released g^{-1} dry soil h^{-1}) as compared to T_2 (113.51 μg p-nitrophenol released g^{-1} dry soil h^{-1}). The trend was similar for nano-Fe, where the level of doses significantly affected the ACP activity as observed in T_4 (87.16 μg p-nitrophenol released g^{-1} dry soil h^{-1}) and T_5 (77.64 μg p-nitrophenol released g^{-1} dry soil h^{-1}).

The pattern of AKP activity in soil amended with nanomaterials was significantly affected by the treatments. In this study, application of nano-Zn at various levels (10 and 40 mg kg^{-1}) significantly affected the AKP; there was a sharp decline (~25%) in the AKP activity when a higher dose of nano-Zn (T_3) was used (Figure 5). FDA activity in soil samples on 0 d ranged from 18.08 in T_5 to 31.63 μg fluorescein released g^{-1} dry soil h^{-1} in the control. FDA activity was significantly decreased when the concentration of nano-Fe was increased from 10 mg kg^{-1} (22.37 μg fluorescein released g^{-1} dry soil h^{-1}) to 40 mg kg^{-1} (18.08 μg fluorescein released g^{-1} dry soil h^{-1}) (at $p < 0.05$). The impact of heat stress sharply reduced FDA activity, which was evident 1 d after incubation (DAI). Across the treatments, data revealed a reduction of the FDA activity by 53 to 84% 1 DAI. The least reduction was in T_2 , with 53%, whereas the control treatment showed the greatest reduction of 84% in FDA activity after heat stress.

Application of nanomaterials showed 24–40% lower MBC than the control on 0 d, while there was no significant difference between the various levels of each nanomaterial used in the experiment. Comparable values were obtained with both the levels of Zn T_2 (158.42 $\mu\text{g g}^{-1}$ dry soil) and T_3 (161.36 $\mu\text{g g}^{-1}$ dry soil). A similar trend was also found with different Fe levels in T_4 (145.47 $\mu\text{g g}^{-1}$ dry soil) and T_5 (142.81 $\mu\text{g g}^{-1}$ dry soil).

Resistance indices of dehydrogenase activity against heat stress showed that T_3 gave the greatest stress resistance (Table 1), with an index rating of 0.70. The control had a greater resistance index with respect to ACP activity. Resistance indices varied from as low as 0.25 in the control treatment to as much as 0.73 in T_3 (Table 1). Although all the treatments varied in terms of the response of AKP activity in the soil, the resistance indices showed a wide variation in terms of the materials used and

their concentrations. Resistance index value for AKP ranged from 0.30 in the control to 0.66 in T₂ (Table 1). Comparable resistance indices were obtained at the concentrations of nano-Fe in both T₄ (0.49) and T₅ 0.52. Stress of high temperature, as in our experiment, drastically reduced the activity of AKP activity. With respect to resistance of FDA activity against heat stress, it was observed that the T₂ and T₄ treatments showed the greatest stress resistance, with index ratings of 0.48 and 0.43, respectively (Table 1). With respect to resistance indices of MBC against heat stress, it was observed that the T₅ treatment showed the greatest stress resistance, with an index rating of 0.69, which was statistically comparable to those of T₃ (0.68) and T₄ (0.67) (Table 1).

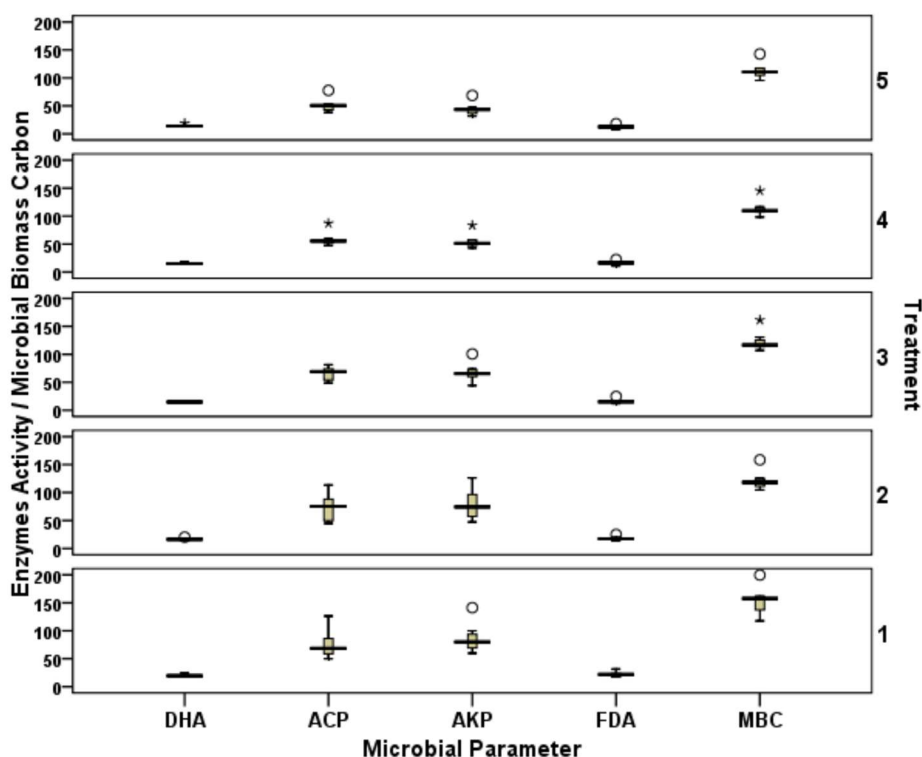


Figure 5. Effect of heat stress on dehydrogenase activity (DHA) ($\mu\text{g TPF released g}^{-1}$ dry soil h^{-1}), acid phosphatase (ACP) activity, alkaline phosphatase (AKP) activity ($\mu\text{g p-nitrophenol released g}^{-1}$ dry soil h^{-1}), fluorescein diacetate activity (FDA) ($\mu\text{g fluorescein released g}^{-1}$ dry soil h^{-1}), and microbial biomass carbon (MBC) ($\mu\text{g g}^{-1}$ dry soil) (secondary Y-axis indicates the treatments 1–5; i.e., T₁ to T₅). The circle represents the values one and half times less than inter-quartile range and asterisks represents the values one and half times more than inter-quartile range. Bars represents the maximum and minimum value.

Table 1. Resistance indices of dehydrogenase (DHA), acid phosphatase (ACP) activity, alkaline phosphatase (AKP) activity, fluorescein diacetate activity (FDA), and microbial biomass carbon (MBC) (mean \pm standard error of mean) in soil after heat stress ($48\text{ }^{\circ}\text{C}$ for 24 hours) under various doses of nanomaterials.

Treatment	DHA	ACP	AKP	FDA	MBC
Control (T ₁)	0.56b (± 0.024)	0.25c (± 0.011)	0.30c (± 0.013)	0.37a (± 0.016)	0.51b (± 0.022)
Nano-Zn @10 mg kg^{-1} (T ₂)	0.69a (± 0.030)	0.58b (± 0.025)	0.66a (± 0.029)	0.48a (± 0.021)	0.59ab (± 0.025)
Nano-Zn @40 mg kg^{-1} (T ₃)	0.70a (± 0.030)	0.73a (± 0.032)	0.58ab (± 0.025)	0.42bc (± 0.018)	0.68a (± 0.029)
Nano-Fe @10 mg kg^{-1} (T ₄)	0.58b (± 0.025)	0.51b (± 0.022)	0.49b (± 0.021)	0.43ab (± 0.019)	0.67a (± 0.029)
Nano-Fe @40 mg kg^{-1} (T ₅)	0.55b (± 0.024)	0.53b (± 0.023)	0.52b (± 0.022)	0.40bc (± 0.017)	0.69a (± 0.030)

Values followed by different letters are significant at $p < 0.05$.

The resilience index showed that the rate of recovery of the DHA was initially rapid (0.32 at 28 d) in the control and then decreased at 70 d (-0.36) after incubation (Table 2). Resilience index ratings at 90 d were 0.21 for T₂, 0.19 for T₃, 0.02 for T₄, and 0.03 for T₅. For ACP, application of nano-Zn showed a resilience index of 0.39 at 10 mg kg^{-1} and 0.40 at 40 mg kg^{-1} nano-Zn concentration. Although the

recovery of ACP activity in the control was faster during the initial incubation (up to 56 d), the trend reversed after 70 d (−0.08) and 90 d (−0.05) of incubation (Table 2). Recovery of AKP was clearly observed after 90 d, with the higher resilience index being observed in T₂ (0.51) and lowest being in T₁ (0.03). It was interesting to observe that the extent of recovery in the treatments T₂ to T₅ were lower during the initial incubation period up to 56 d (−0.05 to −0.43), but started recovering well after 70 d (0.07 to 0.49) and 90 d (0.16 to 0.51) of incubation (Table 2). Recovery of FDA activity following heat stress was clearly observed as early as 14 DAI in all the treatments including the control. This trend was maintained throughout the incubation period except in the control, where there was a slight decline in the recovery at 90 DAI. It was observed that all the treatments supplied with nanomaterials showed a statistically similar resilience of FDA against the heat stress after 90 d (Table 2). Although the control treatment showed a higher resilience index up to 56 d, there was sharp decline in the resilience indices after 70 d (−0.20) and 90 d (−0.01). Recovery rate of MBC showed a similar pattern as the enzymatic activity. Although the resilience indices were lower during the first 56 d, the recovery indices were highest after 90 d of incubation. T₃ and T₅ had the greatest stress resilience, with index ratings of 0.28 and 0.29, respectively, after 90 d of incubation (Table 2).

Table 2. Resilience indices of dehydrogenase activity (DHA), acid phosphatase (ACP) activity, alkaline phosphatase (AKP) activity, fluorescein diacetate activity (FDA), and microbial biomass carbon (MBC) (mean ± standard error of mean) in soil after heat stress (48 °C for 24 h) under various doses of nanomaterials.

Treatment	14 d	28 d	56 d	70 d	90 d
DHA					
T ₁	0.04 ± 0.002	0.32 ± 0.014	0.15 ± 0.006	−0.36 ± 0.016	−0.12 ± 0.005
T ₂	−0.18 ± 0.008	−0.03 ± 0.001	0.06 ± 0.003	0.21 ± 0.009	0.21 ± 0.009
T ₃	−0.05 ± 0.002	0.49 ± 0.021	0.04 ± 0.002	−0.03 ± 0.001	0.19 ± 0.008
T ₄	0.09 ± 0.004	0.24 ± 0.010	0.29 ± 0.013	−0.04 ± 0.002	0.02 ± 0.001
T ₅	0.07 ± 0.003	0.12 ± 0.005	0.20 ± 0.009	−0.07 ± 0.003	0.03 ± 0.001
ACP					
T ₁	0.44 ± 0.019	0.14 ± 0.006	0.20 ± 0.009	−0.08 ± 0.003	−0.05 ± 0.002
T ₂	0.17 ± 0.007	−0.12 ± 0.005	−0.34 ± 0.015	0.38 ± 0.016	0.39 ± 0.017
T ₃	0.04 ± 0.002	0.58 ± 0.025	−0.35 ± 0.015	0.45 ± 0.019	0.40 ± 0.017
T ₄	−0.18 ± 0.008	−0.05 ± 0.002	−0.06 ± 0.003	0.19 ± 0.008	0.15 ± 0.006
T ₅	−0.18 ± 0.008	−0.06 ± 0.003	−0.06 ± 0.003	0.09 ± 0.004	0.24 ± 0.010
AKP					
T ₁	0.29 ± 0.013	0.17 ± 0.007	0.1 ± 0.004	−0.04 ± 0.002	0.03 ± 0.001
T ₂	−0.14 ± 0.006	−0.34 ± 0.015	−0.43 ± 0.019	0.49 ± 0.021	0.51 ± 0.022
T ₃	−0.13 ± 0.006	−0.06 ± 0.003	−0.18 ± 0.008	0.22 ± 0.010	0.36 ± 0.016
T ₄	−0.18 ± 0.008	−0.06 ± 0.003	0.05 ± 0.002	0.07 ± 0.003	0.16 ± 0.007
T ₅	−0.2 ± 0.009	−0.06 ± 0.003	−0.07 ± 0.003	0.21 ± 0.009	0.26 ± 0.011
FDA					
T ₁	0.06 ± 0.003	0.35 ± 0.015	0.23 ± 0.010	−0.20 ± 0.009	−0.01 ± 0.002
T ₂	0.06 ± 0.003	0.25 ± 0.011	0.13 ± 0.006	0.03 ± 0.001	0.15 ± 0.006
T ₃	0 ± 0.001	0.15 ± 0.006	0.18 ± 0.008	−0.02 ± 0.001	0.12 ± 0.005
T ₄	0.25 ± 0.011	0.2 ± 0.009	0.21 ± 0.009	0 ± 0.001	0.14 ± 0.006
T ₅	0.23 ± 0.010	0.19 ± 0.008	0.17 ± 0.007	0.03 ± 0.001	0.16 ± 0.007
MBC					
T ₁	−0.12 ± 0.005	0.03 ± 0.001	0.21 ± 0.009	−0.26 ± 0.011	−0.25 ± 0.011
T ₂	−0.08 ± 0.003	0.08 ± 0.003	0.1 ± 0.004	0.08 ± 0.003	0.14 ± 0.006
T ₃	−0.15 ± 0.006	−0.19 ± 0.008	−0.18 ± 0.008	0.24 ± 0.010	0.28 ± 0.012
T ₄	−0.15 ± 0.006	−0.08 ± 0.003	−0.11 ± 0.005	0.13 ± 0.006	0.24 ± 0.010
T ₅	0 ± 0.003	−0.11 ± 0.005	−0.15 ± 0.006	0.22 ± 0.010	0.29 ± 0.013

T₁: control, T₂: nano-Zn @10 mg kg^{−1}, T₃: nano-Zn @40 mg kg^{−1}, T₄: nano-Fe @10 mg kg^{−1}, T₅: nano-Fe @40 mg kg^{−1}.

3.3. Microbial Counts

Exposure to higher temperature caused a sharp decline in the Actinobacteria count after 1 d of stress (T_2 : 12.33×10^5 colony forming unit (cfu) g^{-1} soil; T_3 : 12.66×10^5 cfu g^{-1} soil, T_4 : 20×10^5 cfu g^{-1} soil, and T_5 : 18×10^5 cfu g^{-1} soil). At 0 d, the density of the fungal population ranged from 17×10^4 to 24×10^4 cfu g^{-1} soils. Data showed that the fungal count with the T_4 (23.67×10^4 cfu g^{-1}) treatment was significantly ($p < 0.05$) higher than the other treatments (Figure 6). Exposure to higher temperature (48 °C in this study) revealed a steep decrease in the fungal population after 1 d of heat stress. The abundance of *Pseudomonas* was also significantly ($p < 0.05$) affected by the application of nanomaterials. Data showed that T_2 (28×10^4 cfu g^{-1}) and T_3 (24.33×10^4 cfu g^{-1}) treatments were similar ($p < 0.05$) in terms of the *Pseudomonas* population, while the data obtained from T_4 (18.33×10^4 cfu g^{-1}) and T_5 (14.33×10^4 cfu g^{-1}) were statistically significantly different. Analysis of the data revealed a *Pseudomonas* reduction of 42% in T_2 (nano-Zn @ 10 mg kg^{-1})-treated soil to 45% with nano-Fe @ 10 mg kg^{-1} (T_4). Higher concentration of metal-oxide nanoparticles (T_3 and T_5) caused a sharp reduction of 30 and 87%, respectively, in the population of *Pseudomonas* (Figure 6). *Azotobacter* population was found to be around 31% lower in treatments supplemented with Zn nanomaterials. The abundance of *Azotobacter* was highest in T_5 (12.67×10^4 cfu g^{-1} soil), followed by T_4 (12×10^4 cfu g^{-1} soil), T_1 (control: 11.33×10^4 cfu g^{-1} soil), T_2 (nano-Zn@ 10 mg kg^{-1} : 8.67×10^4 cfu g^{-1} soil), and T_3 (nano-Zn@ 40 mg kg^{-1} : 8.67×10^4 cfu g^{-1} soil); however, statistical comparison revealed that the doses of nanomaterial were not affecting the *Azotobacter* count in soils (Figure 6).

Data on the resistance index of Actinobacteria revealed that T_4 had the higher index rating of 0.50, followed by T_5 (0.47), T_3 (0.25), and T_2 (0.23). Fungi bear a greater capacity to withstand temperature stress under the application of nano-Fe (both at 10 and 40 mg kg^{-1}). Resistance indices varied from as low as in the control (T_1 : 0.27) to as much as in T_5 (0.52). Resistance index of T_2 and T_3 were found to be 0.39 and 0.28, respectively (Table 3). For *Pseudomonas*, the resistance index was 0.44 in the control (T_1) treatment, 0.54 in T_2 , 0.62 in T_3 , 0.53 in T_4 , and 0.37 in T_5 . Studies on resistance of *Azotobacter* against heat stress revealed that heat stress produced a reduction in the population of *Azotobacter* in all the treatments. The magnitude of decline in the population of *Azotobacter* was higher in the control, as reflected by its lower resistance index rating of 0.26 as compared to other treatments. Application of nano-Fe@ 40 mg kg^{-1} (T_5) showed a resistance index rating of 0.65, which was statistically significant in comparison to other treatments (Table 3).

Table 3. Resistance indices of Actinobacteria, fungi, *Pseudomonas*, and *Azotobacter* (mean \pm standard error of mean) in soil after heat stress (48 °C for 24 hours) under various doses of nanomaterials.

Treatment	Actinobacteria	Fungi	<i>Pseudomonas</i>	<i>Azotobacter</i>
Control (T_1)	0.31b (± 0.013)	0.27c (± 0.012)	0.44bc (± 0.019)	0.26c (± 0.011)
Nano-Zn @10 mg kg^{-1} (T_2)	0.23b (± 0.010)	0.39b (± 0.017)	0.54ab (± 0.023)	0.30c (± 0.013)
Nano-Zn @40 mg kg^{-1} (T_3)	0.25b (± 0.011)	0.28c (± 0.012)	0.62a (± 0.027)	0.24c (± 0.010)
Nano-Fe @10 mg kg^{-1} (T_4)	0.50a (± 0.022)	0.51a (± 0.022)	0.53ab (± 0.023)	0.53b (± 0.023)
Nano-Fe @40 mg kg^{-1} (T_5)	0.47a (± 0.020)	0.52a (± 0.022)	0.37c (± 0.016)	0.65a (± 0.028)

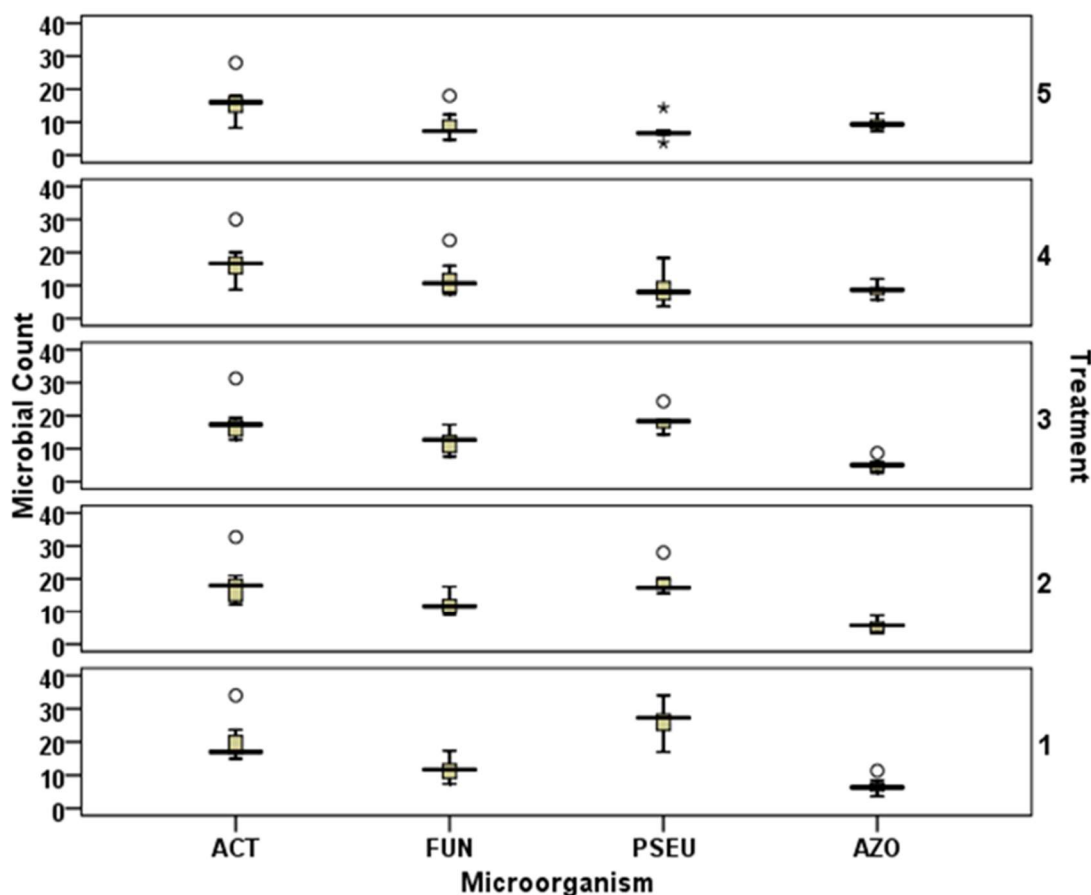


Figure 6. Effect of heat stress on Actinobacteria (ACT) ($\times 10^5$ colony forming unit (cfu) g^{-1} dry soil), fungal (FUN) ($\times 10^4$ cfu g^{-1} dry soil), *Pseudomonas* (PSEU) ($\times 10^4$ cfu g^{-1} dry soil), and *Azotobacter* (AZO) ($\times 10^4$ cfu g^{-1} dry soil) counts (secondary Y-axis indicates the treatments 1–5; i.e., T₁ to T₅). The circle represents the values one and half times less than inter-quartile range and asterisks represents the values one and half times more than inter-quartile range. Bars represents the maximum and minimum value.

Recovery from heat stress by Actinobacteria was clearly observed with nano-Fe (at both doses: 10 and 40 mg kg^{-1}) 90 DAI. Recovery rate of Actinobacteria showed that the resilience index was positive with the application of nano-Fe after 90 DAI (0.36 in T₄ and 0.33 in T₅). Recovery with the addition of Zn nanoparticles followed the same pattern as that of the control after 90 d (Table 4). The recovery rate showed a positive value in all the three treatments (T₁, T₂, and T₃) up to 56 d (0.02–0.27), but there was a decline in those indices (−0.03 for T₁, −0.04 for T₂, and −0.03 for T₃) on 90 DAI. Resilience pattern of fungal population in fertilized treatment showed a positive value in T₂, T₄, and T₅ after 90 d, reflecting the possibility of recovery after the stress (Table 4). Although it is not as close to +1, there are chances that the fungal population will withstand the higher temperature in the future. Resilience index was higher in the T₅ (nano-Fe @ 40 mg kg^{-1}) treatment, with an index rating of 0.40. Recovery after heat stress by *Pseudomonas* was clearly observed 90 DAI. The rate of such a recovery of *Pseudomonas* was in the order T₄ > T₃ > T₅ > T₂ > T₁ at $p < 0.05$. T₄ showed the higher resilience index rating of 0.43, followed by T₃ (0.24) and T₅ (0.23) (Table 4).

Regarding the resilience of *Azotobacter*, it was observed that the T₅ (nano-Fe @ 40 mg kg^{-1}) treatment had the highest resilience (0.33) of all the treatments at 90 d of incubation.

Table 4. Resilience indices of Actinobacteria, fungi, *Pseudomonas*, and *Azotobacter* (mean \pm standard error of mean) in soil after heat stress (48 °C for 24 hours) under various doses of nanomaterials.

Treatment	14 d	28 d	56 d	70 d	90 d	14 d	28 d	56 d	70 d	90 d
	<i>Actinobacteria</i>					<i>Fungi</i>				
T ₁	0.27 \pm 0.012	0.13 \pm 0.006	0.02 \pm 0.001	0.02 \pm 0.001	−0.03 \pm 0.001	0.43 \pm 0.019	0.43 \pm 0.019	0.28 \pm 0.012	−0.09 \pm 0.004	−0.09 \pm 0.004
T ₂	0.16 \pm 0.007	0.27 \pm 0.012	0.18 \pm 0.008	−0.01 \pm 0.000	−0.04 \pm 0.002	0.44 \pm 0.019	0.21 \pm 0.009	0.12 \pm 0.005	0.06 \pm 0.003	0.04 \pm 0.002
T ₃	0.17 \pm 0.007	0.22 \pm 0.010	0.14 \pm 0.006	−0.04 \pm 0.002	−0.03 \pm 0.001	0.53 \pm 0.023	0.45 \pm 0.019	0.35 \pm 0.015	−0.05 \pm 0.002	−0.08 \pm 0.003
T ₄	−0.13 \pm 0.006	−0.14 \pm 0.006	−0.21 \pm 0.009	0.28 \pm 0.012	0.36 \pm 0.016	−0.25 \pm 0.011	−0.24 \pm 0.010	−0.33 \pm 0.014	0.35 \pm 0.015	0.36 \pm 0.016
T ₅	−0.03 \pm 0.001	−0.14 \pm 0.006	−0.09 \pm 0.004	0.25 \pm 0.011	0.33 \pm 0.014	−0.22 \pm 0.010	−0.31 \pm 0.013	−0.32 \pm 0.014	0.31 \pm 0.013	0.40 \pm 0.017
	<i>Pseudomonas</i>					<i>Azotobacter</i>				
T ₁	−0.12 \pm 0.005	0.03 \pm 0.001	0.36 \pm 0.016	−0.45 \pm 0.019	−0.27 \pm 0.012	0.14 \pm 0.006	0.18 \pm 0.008	0.38 \pm 0.016	−0.11 \pm 0.005	0.07 \pm 0.003
T ₂	−0.19 \pm 0.008	−0.12 \pm 0.005	−0.12 \pm 0.005	−0.04 \pm 0.002	0.15 \pm 0.006	−0.03 \pm 0.001	0.55 \pm 0.024	0.27 \pm 0.012	−0.22 \pm 0.010	0.07 \pm 0.003
T ₃	−0.27 \pm 0.012	−0.03 \pm 0.001	0 \pm 0.004	0.08 \pm 0.003	0.24 \pm 0.010	0.03 \pm 0.001	0.18 \pm 0.008	0.33 \pm 0.014	−0.19 \pm 0.008	0.06 \pm 0.003
T ₄	−0.21 \pm 0.009	−0.29 \pm 0.013	−0.32 \pm 0.014	0.44 \pm 0.019	0.43 \pm 0.019	0.05 \pm 0.002	0.10 \pm 0.004	0.22 \pm 0.010	0.27 \pm 0.012	0.24 \pm 0.010
T ₅	−0.07 \pm 0.003	−0.05 \pm 0.002	−0.07 \pm 0.003	0.09 \pm 0.004	0.23 \pm 0.010	0.33 \pm 0.014	−0.24 \pm 0.010	−0.11 \pm 0.005	0.27 \pm 0.012	0.33 \pm 0.014

T₁: Control, T₂: nano-Zn (n-Zn) @10 mg kg^{−1}, T₃: n-Zn @40 mg kg^{−1}, T₄: n-Fe @10 mg kg^{−1}, T₅: n-Fe @40 mg kg^{−1}.

3.4. Microbial Correlations

Correlation studies signify the role of interaction between Actinobacteria, *Azotobacter*, and fungi for fabricating the resistance against heat stress (Table 5). It is clear that Actinobacteria had a positive and highly significant correlation with *Azotobacter* ($r = 0.904$, $p < 0.01$), and even the fungi are well correlated with *Azotobacter* ($r = 0.937$, $p < 0.01$). Recovery of the microorganism and soil enzymes can be attributed to the predominant role of Actinobacteria interacting with fungi ($r = 0.869$, $p < 0.01$), *Pseudomonas* ($r = 0.422$, $p < 0.05$), and *Azotobacter* ($r = 0.516$, $p < 0.01$) (Table 5).

Table 5. Pearson correlation matrix among enzyme activity, microbial biomass carbon, and microbial population, considering the data of the resistance indices calculated following the first day of stress and the resilience indices calculated over the whole period of the study.

Resistance Indices									
	DHA	ACP	AKP	FDA	MBC	Actino	Fungi	Pseudo	Azo
DHA	1								
ACP	0.727	1							
AKP	0.735	0.865	1						
FDA	0.691	0.595	0.876	1					
MBC	0.114	0.761	0.545	0.224	1				
Actino	−0.775	−0.203	−0.273	−0.299	0.462	1			
Fungi	−0.440	0.113	0.254	0.236	0.583	0.819	1		
Pseudo	0.846	0.628	0.484	0.528	0.168	−0.526	−0.415	1	
Azo	−0.638	−0.005	0.031	−0.091	0.584	0.904*	0.937*	−0.612	1

Resilience Indices									
	DHA	ACP	AKP	FDA	MBC	Actino	Fungi	Pseudo	Azo
DHA	1								
ACP	0.294	1							
AKP	0.205	0.753 **	1						
FDA	0.666 **	−0.207	−0.186	1					
MBC	0.062	0.380	0.463 *	0.128	1				
Actino	−0.259	0.202	−0.018	−0.137	0.323	1			
Fungi	−0.116	0.348	0.095	−0.094	0.225	0.869 **	1		
Pseudo	0.178	0.422 *	0.445	0.182	0.784 **	0.422 *	0.369	1	
Azo	0.061	−0.240	−0.285	0.438 *	0.284	0.516 **	0.401 *	0.309	1

DHA:dehydrogenase activity; ACP:acid phosphatase activity; AKP:alkaline phosphatase activity; FDA:fluorescein diacetatehydrolyzing capacity; MBC:microbial biomass carbon; Actino:Actinobacteria; Pseudo:Pseudomonas; Azo:Azotobacter; *Correlation is significant at $p < 0.05$; ** Correlation is significant at $p < 0.01$.

4. Discussion

The response of microbial populations and associated enzymes to exogenous stimuli (nano-Fe and -Zn application) is a promising field of study globally, and this experiment was designed to evaluate the impact of synthetic nanomaterials on the buffering of biological activity after heat stress, despite their current application as a smart delivery system for controlled-release formulations [24].

The overall soil DHA, an oxidoreductase enzyme, transfers protons and electrons from substrates to acceptors, is a fundamental part of the enzyme system of all living soil microorganisms and reflects the oxidative capacities of microbes. Results revealed that the metal-oxide nanomaterials confer higher microbial resistance in lower concentrations than with higher concentrations. Heavy metals interact with the enzyme–substrate complex or with the protein active groups and thereby reduce enzyme activity by denaturing the enzyme protein [25]. There was 30% and 12.5% reduction in the DHA at a Zn concentration of 50 mg kg^{-1} [26] and nano-ZnO applied at the rate of 1000 mg kg^{-1} , respectively [27]. Additionally, higher Fe_2O_3 concentration acts as an alternate electron acceptor to hydrogen, due to which the dehydrogenase activity might have fallen down, hence exhibiting lower resistance. From the enzymatic data on resilience, it is clear that the treatments of nano-Zn@10 mg kg^{-1} slowly recovered after disturbance, but that rate of recovery was much higher after 90 d. The interaction of enzymes with soil colloids governs the resistance of enzymes and resilience being controlled by those organisms

that survived in the later stages after heat stress and were capable of producing new enzymes [16]. Phosphatases are a broad group of enzymes that hydrolyze esters and anhydrides of phosphoric acid and provide P for plant uptake by releasing PO_4^{3-} from immobile organic P. The ACP was much lower than AKP irrespective of the treatments, which may be due to the alkaline reaction of the soil as reported by soil pH. There are studies that reported elevated phosphatase enzyme activities as a result of metals present in the soil that serve as the cofactors or activators. However, addition of nanomaterials resulted in lower rather than higher enzyme activities after the stress, probably by denaturing the protein, forming a complex with the substrate, or by reacting with the enzyme substrate complex [28]. However, after having conducted the analysis in the subsequent interval, it is clear that the nanomaterials or the soil themselves are not activating the enzymes studied and something else might be responsible for the partial recovery of phosphatase activities as observed in the soil samples [29]. However, experimental data obtained in the laboratory may not fully reflect what happens in soil, being a heterogeneous unit. Resistance index for most of the cases indicated that introduction of nanomaterials (Fe and Zn) provided higher resistance with respect to control soil. Adsorption of free enzymes onto nano-ZnO and $-\text{Fe}_2\text{O}_3$ materials (nano-Fe and -Zn) provided higher thermal stability and hydrolytic stability [30], and therefore providing better resistance when subjected to heat stress. Enhanced thermal stability of enzymes after adsorption might be attributed to the loss of its conformational flexibility [31], as the immobilized enzyme becomes stiff and maintains its stability at higher temperature [32]. The stability of immobilized enzyme is proportional to the ratio of physical adsorption between the enzyme and the support, which lock the enzyme into the active conformation [33]. The FDA hydrolysis in soils represents the activity of a group of enzymes including proteases, lipases, and esterases [19]. In this study, addition of nanomaterials either at 10 or 40 mg kg^{-1} did not have much effect on the resistance index (0.48 and 0.43 for nano-Zn@ 10 mg kg^{-1} and nano-Fe@ 10 mg kg^{-1} , respectively). However, inhibition of the hydrolyzing capacity of FDA may be ascribed to the changes in the molecular structure. Previous reports confirm the probable reaction with sulfhydryl group of enzymes and formation of metal sulfides thereby inactivating the enzyme activity [34]. Lack of resilience of FDA up to 56 d in soil suggests that the addition of nanomaterials caused a temporal reduction in microbial diversity. However, it attains a resilience value ranging from 0.12 to 0.16 after 90 d of incubation. In general, exogenous application of nanomaterials (Zn and Fe) causes a decline in soil enzymatic activities with respect to control soil due to higher adsorption of extracellular free enzymes onto surface of nanomaterials (Fe and Zn). Higher application dose (40 mg kg^{-1}) resulted in greater decline in enzymatic activity with respect to the lower application dose (10 mg kg^{-1}), which may be attributed to higher specific surface area resulting in higher adsorption. The Fe nanoparticles caused greater decline in enzymatic activity as compared to Zn at the same application dose, owing to the smaller particle size of the former (40–50 nm) (Figures 1 and 2) with respect to the latter (50–60 nm) (Figures 1 and 2), causing more desorption of free enzymes.

Soil MBC implies the soil microbial population and can be used as an indicator to evaluate the impact of stress on microorganisms and associated enzymes in soils [35]. Exposure to higher temperature causes shock, cytoplasm leakage, and lysis of the microorganisms. Zn has also been validated to reduce the size of the soil microbial biomass [36]. The role of extracellular polymeric substances (EPS), a high-molecular-weight mixture of polymers, in trapping the nanoparticles outside the cells exhibiting resistance to toxicity is well explained [37,38]. Previous data indicates that the reduction of microbial biomass with nano-Fe was primarily due to reduced Gram-negative bacteria, which include *Pseudomonas* [7]. When taken collectively, the results of the current study clearly indicate that the impact of nanoparticles on microbial population may be dependent on the heat stress applied rather than the properties of soil. Nevertheless, there is the possibility that these materials undergo chemical transformations such as oxidation, ionization, etc. [39], but their assessment on microbial populations strongly confirms an initial sharp decrease. Environmental parameters may largely influence the rate of chemical transformation of nanoparticles, and depending on whether the microbial toxicity of nanoparticles is through direct or indirect interaction with the cells, the fate determines the

impact of nanoparticles on the soil microbial community [40]. Fe is an essential nutrient for almost all microorganisms as it is a cofactor for a large number of enzymes that play an important role in many biochemical reactions, including respiration and DNA synthesis. Microorganisms employ various Fe uptake mechanisms to ensure sufficient supplies from their surroundings [41]. Resilience in the count of microorganisms in nano-Fe-treated soil reflected that Fe possibly took part in the metabolic reactions and provided beneficial nutrients essential for the growth of some microbes in soil. Few studies have confirmed the role of ROS in imparting the toxicity effect of Fe-based nanoparticles. The Fe₂O₃ nanoparticles are highly stable in the environment, and thus have a lower capacity to generate oxidative stress. Therefore, the decline in cultivable population during the early stage can only be attributed to the exposure of soil to higher temperature. Studies with nano-zero-valent Fe induces modification of the soil microbial community [7], including bacterial and fungal populations in the short term (less than 4 months), but our study contradicts the related decrease with nano-Fe over the 90-d study period. This might be due to the fact that Fe-nanoparticles stimulated the population of several bacteria related to Actinobacteria, such as *Duganella*, Streptomycetaceae, or *Nocardioideis*, and suggests the improved resistance and resilience of microorganisms reported in this study [42]. *Pseudomonas* has a specific mechanism to form resting spores to overcome abiotic stress such as heat [43]. Thus, they possess higher resistance value than *Azotobacter* and Actinobacteria. Griffiths et al. [44] suggested that functional resistance of *P. fluorescens* in different soils in response to heat stress ranged from 10–68% as compared to the unstressed control. Research has confirmed that nano-zero-valent Fe exerts a selective pressure on the microbial community [45], promoting the dominance of some microbial groups (Archaea, α -Proteobacteria, and low G+C Gram-positive bacteria) or the decrease of other ones (β - and γ -Proteobacteria and subclasses). *Azotobacter* is a typical mesophilic bacterium for which the optimum temperature for growth ranges between 25–30 °C; however, the minimum temperature for *Azotobacter* growth evidently lies a little above 0 °C. Vegetative *Azotobacter* cells cannot tolerate high temperatures, and if kept at 55–60 °C, they degenerate and die [46]. *Azotobacter* cysts are generally produced in the late stationary phase or upon induction of vegetative cells with specific reagents [47], which confirms the resilience of the population as observed after 90 d of incubation. Production of the late embryogenesis abundant (LEA) proteins might have played an important role in shielding the proteins and enzymes of *Azotobacter* cells under high-temperature stress [48] and hence recovery thereafter. Other proposed defense mechanisms include trehalose and heat shock proteins (HSPs) that act at high temperatures by preventing protein aggregation, unfolding aggregated proteins, or targeting denatured proteins for degradation [49]. Heat tolerance is known to be key to fungal survival in stressed soil, and a recent report confirmed the role of pyruvate in the scavenging of heat-induced ROS: the α -keto-carboxylate structure in pyruvate neutralizes peroxides by reducing them to their conjugate alcohols, along with the decomposition of pyruvate into acetate and CO₂ [50].

Our correlation studies showed a number of interactions of Actinobacteria with other microorganisms which drive the resistance and resilience of the experimental soil. These interactions ecologically improved the fitness of soils to resist the stress through mechanisms such as producing some specific genes linked to cell–cell interaction, affecting changes in the metabolic mechanisms and thereby producing the resistance and resilience against the stress [51]. Interaction of *Azotobacter* and fungi leads to the increased growth of fungi through signaling secondary metabolites produced by *Azotobacter*, responsible for combating the stresses [52]. Although this kind of interaction is known to occur in the rhizosphere region, the exact nature of the molecular interaction is yet to be elucidated.

In summary, our results show that the presence of either nanomaterials or the exposure to heat stress decreased the soil enzymatic activities as well as the microbial counts. Soil enzymatic activities studied in the current experiment clearly reflected the explicit role of Zn nanomaterials in improving its resistance as well as resilience after 90 d of the experiment. The pattern of microbial counts varied over the study period, and Fe nanomaterial was found to aid the recovery of organisms 90 d after heat stress. The erratic pattern observed in the biological parameters indicated that nanomaterials might hamper these enzymes or microbial count in its initial segment of incubation, but that they do have the

competency to recover within 90 d, as observed in the current study. Since the present scope of study was limited to investigations carried out under controlled laboratory conditions, we acknowledge that the actual scenario may be different under the field situation, where apart from varying climatic factors, several other factors may also interact in a complex way. Further, it is necessary to conduct additional investigation of the long-term effects of nanoparticles before drawing a comprehensive conclusion about the effects of nanoparticles on the soil microbial ecosystem.

Author Contributions: Conceptualization, R.R.; Methodology, A.K., N.M. and S.A.; Formal Analysis, A.D.; Writing-Original Draft Preparation, R.R.; Writing-Review & Editing, A.B. and A.D.

Funding: This research received no external funding.

Acknowledgments: Authors are thankful to the Vice Chancellor, Bihar Agricultural University (BAU), Bhagalpur, Bihar, India, for providing necessary facilities, and the Director of Research, BAU, for his support and critical suggestions. Special thanks are given to the scientists associated with All India Coordinated Research Project-Integrated Farming System, Sabour unit, and North Carolina A&T State University, USA. Authors are thankful for the contribution made by V.K. Barnwal, Principal Scientist, Plant Virology Unit, Division of Plant Pathology, IARI, New Delhi, in providing the TEM images for the synthesized nanomaterials. Sincere thanks are given to S.C. Datta, Principal Scientist, Division of Soil Science and Agricultural Chemistry, IARI, New Delhi, for providing the necessary facilities for obtaining the XRD images of the materials.

Conflicts of Interest: The authors declare no conflict of interest.

References

1. Wang, Z.; Lee, Y.H.; Wu, B.; Horst, A.; Kang, Y.; Tang, Y.J.; Chen, D.R. Anti-microbial activities of aerosolized transition metal oxide nanoparticles. *Chemosphere* **2010**, *80*, 525–529. [[CrossRef](#)] [[PubMed](#)]
2. Tourinho, P.S.; van Gestel, C.A.; Lofts, S.; Svendsen, C.; Soares, A.M.; Loureiro, S. Metal-based nanoparticles in soil: Fate, behavior, and effects on soil invertebrates. *Environ. Toxicol. Chem.* **2012**, *31*, 1679–1692. [[CrossRef](#)]
3. Dinesh, R.; Anandaraj, M.; Srinivasan, V.; Hamza, S. Engineered nanoparticles in the soil and their potential implications to microbial activity. *Geoderma* **2012**, *173*, 19–27. [[CrossRef](#)]
4. Jiang, W.; Mashayekhi, H.; Xing, B. Bacterial toxicity comparison between nano- and micro-scaled oxide particles. *Environ. Pollut.* **2009**, *157*, 1619–1625. [[CrossRef](#)] [[PubMed](#)]
5. Dimkpa, C.O.; Calder, A.; Britt, D.W.; McLean, J.E.; Anderson, A.J. Responses of a soil bacterium, *Pseudomonas chlororaphis* O6 to commercial metal oxide nanoparticles compared with responses to metal ions. *Environ. Pollut.* **2011**, *159*, 1749–1756. [[CrossRef](#)] [[PubMed](#)]
6. Xia, T.; Kovoichich, M.; Liong, M.; Madler, L.; Gilbert, B.; Shi, H.; Yeh, J.I.; Zink, J.I.; Nel, A.E. Comparison of the mechanism of toxicity of zinc oxide and cerium oxide nanoparticles based on dissolution and oxidative stress properties. *ACS Nano* **2008**, *2*, 2121–2134. [[CrossRef](#)] [[PubMed](#)]
7. Pawlett, M.; Ritz, K.; Dorey, R.A.; Rocks, S.; Ramsden, J.; Harris, J.A. The impact of zero-valent iron nanoparticles upon soil microbial communities is context dependent. *Environ. Sci. Pollut. Res.* **2013**, *20*, 1041–1049. [[CrossRef](#)]
8. Cullen, L.G.; Tilston, E.L.; Mitchell, G.R.; Collins, C.D.; Shaw, L.J. Assessing the impact of nano- and micro-scale zerovalent iron particles on soil microbial activities: Particle reactivity interferes with assay conditions and interpretation of genuine microbial effects. *Chemosphere* **2011**, *82*, 1675–1682. [[CrossRef](#)]
9. Rakshit, R.; Patra, A.K.; Pal, D.; Kumar, M.; Singh, R. Effect of elevated CO₂ and temperature on nitrogen dynamics and microbial activity during wheat (*Triticum aestivum* L.) growth on a subtropical Inceptisol in India. *J. Agron. Crop Sci.* **2012**, *198*, 452–465. [[CrossRef](#)]
10. Pimm, S.L. The complexity and the stability of ecosystems. *Nature* **1984**, *307*, 321–326. [[CrossRef](#)]
11. Griffiths, B.S.; Bonkowski, M.; Roy, J.; Ritz, K. Functional stability, substrate utilisation and biological indicators of soils following environmental impacts. *Appl. Soil Ecol.* **2001**, *16*, 49–61. [[CrossRef](#)]
12. Aneesh, P.M.; Vanaja, K.A.; Jayaraj, M.K. Synthesis of ZnO nanoparticles by hydrothermal method. Nanophotonic Materials IV, edited by Zeno Gaburro, Stefano Cabrini. *Proc. SPIE* **2007**, *6639*, 66390J. [[CrossRef](#)]
13. Shah, M.A.; Shah, K.A. *Nanotechnology: The Science of Small*; The Wiley India Pvt. Ltd.: Noida, India, 2013; p. 167.

14. Hubbard, C.R. *National Bureau of Standards Monograph 25 Section 18-Data for 58 Substances Nat. Bur. Stand. (U.S.), Monogr. 25–Sec. 18*; International Centre for Diffraction Data: Newtown Square, PA, USA, 1981.
15. Hall, B.D.; Zanchet, D.; Ugarte, D. Estimating nanoparticle size from diffraction measurements. *J. Appl. Crystallogr.* **2000**, *33*, 121–132. [[CrossRef](#)]
16. Kumar, S.; Patra, A.K.; Singh, D.; Purakayastha, T.J. Long-term chemical fertilization along with farmyard manure enhances resistance and resilience of soil microbial activity against heat stress. *J. Agron. Crop Sci.* **2014**, *200*, 156–162. [[CrossRef](#)]
17. Klein, D.A.; Loh, T.C.; Goulding, R.L. A rapid procedure to evaluate dehydrogenase activity of soils low in organic matter. *Soil Biol. Biochem.* **1971**, *3*, 385–387. [[CrossRef](#)]
18. Tabatabai, M.A.; Bremner, J.M. Use of *p*-nitrophenyl phosphate for assay of soil phosphatase activity. *Soil Biol. Biochem.* **1969**, *1*, 301–307. [[CrossRef](#)]
19. Green, V.S.; Stott, D.E.; Diack, M. Assay for fluorescein diacetate hydrolytic activity: Optimization for soil samples. *Soil Biol. Biochem.* **2006**, *38*, 693–701. [[CrossRef](#)]
20. Vance, E.D.; Brookes, P.C.; Jenkinson, D.S. An extraction method for measuring soil microbial biomass C. *Soil Biol. Biochem.* **1987**, *19*, 703–707. [[CrossRef](#)]
21. Chhonkar, P.K.; Bhadraray, S.; Patra, A.K.; Purakayastha, T.J. *Experiments in Soil Biology and Biochemistry*; Westville: New Delhi, India, 2007.
22. Orwin, K.H.; Wardle, D.A. New indices for quantifying the resistance and resilience of soil biota to exogenous disturbances. *Soil Biol. Biochem.* **2004**, *36*, 1907–1912. [[CrossRef](#)]
23. Gomez, K.A.; Gomez, A.A. *Statistical Procedures for Agricultural Research*; John Wiley and Sons: New York, NY, USA, 1984.
24. Mandal, N.; Datta, S.C.; Manjaiah, K.M.; Dwivedi, B.S.; Kumar, R.; Aggarwal, P. Zincated nanoclay polymer composites (ZNCPCs): Synthesis, characterization, biodegradation and controlled release behaviour in soil. *Polym. Plast. Technol. Eng.* **2018**, *57*, 1760–1770. [[CrossRef](#)]
25. Pan, J.; Yu, L. Effects of Cd or/and Pb on Soil Enzyme Activities and Microbial Community Structure. *Ecol. Eng.* **2011**, *37*, 1889–1894. [[CrossRef](#)]
26. Wyszowska, J.; Kucharski, J.; Lajszner, W. The effect of copper on soil biochemical properties and its interaction with other heavy metals. *Pol. J. Environ. Stud.* **2006**, *15*, 927–934.
27. Kim, S.; Sin, H.; Lee, S.; Lee, I. Influence of metal oxide particles on soil enzyme activity and bioaccumulation of two plants. *J. Microbiol. Biotechnol.* **2013**, *23*, 1279–1286. [[CrossRef](#)]
28. Hemida, S.K.; Omar, S.A.; Abdel-Mallek, A.Y. Microbial populations and enzyme activities in soil treated with heavy metals. *Water Air Soil Pollut.* **1997**, *95*, 13–22. [[CrossRef](#)]
29. Hagmann, D.F.; Goodey, N.M.; Mathieu, C.; Evans, J.; Aronson, M.F.J.; Gallagher, F.; Krumins, J.A. Effect of metal contamination on microbial enzymatic activity in soil. *Soil Biol. Biochem.* **2015**, *91*, 291–297. [[CrossRef](#)]
30. Bayramoglu, G.; Yalc, E.; Arica, M.Y. Immobilization of urease via adsorption into I-histidine- Ni (II) complexed poly (HEMA-MAH) microspheres: Preparation and characterization. *Process Biochem.* **2005**, *40*, 3505–3513. [[CrossRef](#)]
31. Busto, M.D. An experiment illustrating the effect of immobilization on enzyme properties. *Biochem. Educ.* **1998**, *26*, 304–308. [[CrossRef](#)]
32. Rahman, M.B.A.; Zaidan, U.H.; Basri, M.; Hussein, M.Z.; Rahman, R.N.Z.R.A.; Salleh, A.B. Enzymatic synthesis of methyl adipate ester using lipase from *Canidarugosa* immobilized on Mg, Zn and Ni of layered double hydroxides. *J. Mol. Catal. B Enzym.* **2008**, *50*, 33–39. [[CrossRef](#)]
33. Lenders, J.P.; Germain, P.; Crichton, R.R. Immobilization of a soluble chemically thermostabilized enzyme. *Biotechnol. Bioeng.* **1985**, *27*, 572–578. [[CrossRef](#)]
34. Du, W.; Sun, Y.; Ji, R.; Zhu, J.; Wu, J.; Guo, H. TiO₂ and ZnO nanoparticles negatively affect wheat growth and soil enzyme activities in agricultural soil. *J. Environ. Monit.* **2011**, *13*, 822–828. [[CrossRef](#)]
35. Brookes, P.C. The use of microbial parameters in monitoring soil pollution by heavy metals. *Biol. Fertil. Soils* **1995**, *19*, 269–279. [[CrossRef](#)]
36. Renella, G.; Chaudri, A.M.; Brookes, P.C. Fresh additions of heavy metals do not model long-term effects on microbial biomass and activity. *Soil Biol. Biochem.* **2002**, *34*, 121–124. [[CrossRef](#)]
37. Hong, Z.; Chen, W.; Rong, X.; Cai, P.; Dai, K.; Huang, Q. The effect of extracellular polymeric substances on the adhesion of bacteria to clay minerals and goethite. *Chem. Geol.* **2013**, *60*, 118–125. [[CrossRef](#)]

38. Joshi, N.; Ngwenya, B.T.; French, C.E. Enhanced resistance to nanoparticles toxicity is conferred by overproduction of extracellular polymeric substances. *J. Hazard. Mater.* **2012**, *241*, 363–370. [[CrossRef](#)]
39. Colman, B.P.; Arnaout, C.L.; Anciaux, S.; Gunsch, C.K.; Hochella, M.F., Jr.; Kim, B.; Lowry, G.V.; McGill, B.M.; Reinsch, B.C.; Richardson, C.J.; et al. Low concentrations of silver nanoparticles in biosolids cause adverse ecosystem responses under realistic field scenario. *PLoS ONE* **2013**, *8*, e57189. [[CrossRef](#)] [[PubMed](#)]
40. Reidy, B.; Haase, A.; Luch, A.; Dawson, K.A.; Lynch, I. Mechanism of silver nanoparticle release, transformation and toxicity: A critical review of current knowledge and recommendations for future studies and applications. *Materials* **2013**, *6*, 2295–2350. [[CrossRef](#)] [[PubMed](#)]
41. Hantke, K. Iron and metal regulation in bacteria. *Curr. Opin. Microbiol.* **2001**, *4*, 172–177. [[CrossRef](#)]
42. He, S.; Feng, Y.; Ren, H.; Zhang, Y.; Gu, N.; Lin, X. The impact of iron oxide magnetic nanoparticles on the soil bacterial community. *J. Soils Sediments* **2011**, *11*, 1408–1417. [[CrossRef](#)]
43. Griffiths, B.S.; Philippot, L. Insights into the resistance and resilience of the soil microbial community. *FEMS Microbiol. Rev.* **2013**, *37*, 112–129. [[CrossRef](#)]
44. Griffiths, B.S.; Hallett, P.D.; Kuan, H.L.; Gregory, A.S.; Watts, C.W.; Whitmore, A.P. Functional resilience of soil microbial communities depends on both soil structure and microbial community composition. *Biol. Fertil. Soils* **2008**, *44*, 745–754. [[CrossRef](#)]
45. Fajardo, C.; Ortíz, L.T.; Rodríguez-Membibre, M.L.; Nande, M.; Lobo, M.C.; Martín, M. Assessing the impact of zero-valent iron (ZVI) nanotechnology on soil microbial structure and functionality: A molecular approach. *Chemosphere* **2012**, *86*, 802–808. [[CrossRef](#)]
46. Hogg, S. *Essential Microbiology*; John Wiley and Sons Ltd.: Mangester, UK, 2005.
47. Sutherland, I.W. Biosynthesis and composition of gram-negative bacterial extracellular and wall polysaccharides. *Annu. Rev. Microbiol.* **1985**, *39*, 243–270. [[CrossRef](#)]
48. Rodríguez-Salazar, J.; Moreno, S.; Espin, G. LEA proteins are involved in cyst desiccation resistance and other abiotic stresses in *Azotobacter vinelandii*. *Cell Stress Chaperons* **2017**, *22*, 397–408. [[CrossRef](#)] [[PubMed](#)]
49. Verghese, J.; Abrams, J.; Wang, Y.; Morano, K.A. Biology of the heat shock response and protein chaperones: Budding yeast (*Saccharomyces cerevisiae*) as a model system. *Microbiol. Mol. Biol. Rev.* **2012**, *76*, 115–158. [[CrossRef](#)] [[PubMed](#)]
50. Zhang, X.; St Leger, R.J.; Fang, W. Pyruvate accumulation is the first line of cell defense against heat stress in a fungus. *mBio* **2017**, *8*, e01284-17. [[CrossRef](#)] [[PubMed](#)]
51. Deveau, A.; Barret, M.; Diedhiou, A.G.; Leveau, J.; de Boer, W.; Martin, F.; Sarniguet, A.; Frey-Klett, P. Pairwise transcriptomic analysis of the interactions between the ectomycorrhizal fungus *Laccaria bicolor* S238N and three beneficial, neutral and antagonistic soil bacteria. *Microb. Ecol.* **2015**, *69*, 146–159. [[CrossRef](#)] [[PubMed](#)]
52. Bhuyan, S.K.; Bandyopadhyay, P.; Kumar, P.; Mishra, D.K.; Prasad, R.; Kumari, A.; Upadhyaya, K.C.; Varma, A.; Yadava, P.K. Interaction of *Piriformospora indica* with *Azotobacter chroococcum*. *Sci. Rep.* **2015**, *5*, 13911. [[CrossRef](#)]

